Draft version May 10, 2018
Typeset using LaTeX **manuscript** style in AASTeX62

Electron-ion Recombination Rate Coefficients of Be-like $^{40}Ca^{16+}$

S. X. Wang,[1,2] X. Xu,[1,2] Z. K. Huang,[3] W. Q. Wen,[3] H. B. Wang,[3] N. Khan,[3] S. P. Preval,[4] N. R. Badnell,[5] S. Schippers,[6] S. Mahmood,[3,7] L. J. Dou,[3] X. Y. Chuai,[3] D. M. Zhao,[3] X. L. Zhu,[3] L. J. Mao,[3] X. M. Ma,[3] J. Li,[3] R. S. Mao,[3] Y. J. Yuan,[3] M. T. Tang,[3] D. Y. Yin,[3] J. C. Yang,[3] X. Ma,[3] and L. F. Zhu[1,2]

[1]*Hefei National Laboratory for Physical Sciences at Microscale and Department of Modern Physics, University of Science and Technology of China, Hefei, Anhui 230026, People's Republic of China*

[2]*Synergetic Innovation Center of Quantum Information and Quantum Physics, University of Science and Technology of China, Hefei, Anhui 230026, People's Republic of China*

[3]*Institute of Modern Physics, Chinese Academy of Sciences, 730000 Lanzhou, People's Republic of China*

[4]*Department of Physics and Astronomy, University of Leicester, University Road, Leicester, LE1 7RH, United Kingdom*

[5]*Department of Physics, University of Strathclyde, Glasgow G4 0NG, United Kingdom*

[6]*I. Physikalisches Institut, Justus-Liebig-Universität Gießen, Heinrich-Buff-Ring 16, 35392 Giessen, Germany*

[7]*Physics Division , PINSTECH, Nilore, Islamabda, 45650, Pakistan*

ABSTRACT

Electron-ion recombination rate coefficients for beryllium-like calcium ions in the center of mass energy from 0 to 51.88 eV have been measured by employing the electron-ion merged-beam technique at the cooler storage ring CSRm at the Institute of Modern Physics, Lanzhou, China. The measurement energy range covers the dielectronic recombination (DR) resonances associated with the $2s^2\ ^1S_0 \rightarrow 2s2p\ ^3P_{0,1,2},^1P_1$ core

Corresponding author: W. Q. Wen
wenweiqiang@impcas.ac.cn

Corresponding author: X. Ma
x.ma@impcas.ac.cn

Corresponding author: L. F. Zhu
lfzhu@ustc.edu.cn

excitations and the trielectronic recombination (TR) resonances associated with the $2s^2\ ^1S_0 \rightarrow\ 2p^2\ ^3P_{0,1,2},^1D_2,^1S_0$ core excitations. In addition, theoretical calculations of the recombination rate coefficients have been performed for comparison with the experimental results using the state-of-the-art multi-configuration Breit-Pauli atomic structure code. Resonant recombination originating from parent ions in the long-lived metastable state $2s2p\ ^3P_0$ ions has been identified in the recombination spectrum below 1.25 eV. A good agreement is achieved between the experimental recombination spectrum and the result of the AUTOSTRUCTURE calculations when fractions of 95% ground-state ions and 5% metastable ions are assumed in the calculation. It is found that the calculated TR resonance positions agree with the experimental peaks while the resonance strengths are much underestimated by the theoretical calculation. Temperature dependent plasma rate coefficients for DR and TR in the temperature range $10^3 - 10^8$ K were derived from the measured electron-ion recombination rate coefficients and compared with the available theoretical results from the literature. In the temperature range of photoionized plasmas, the presently calculated rate coefficients and the recent results of Gu (2003) and Colgan et al. (2003) are up to 30% lower than the experimentally derived plasma rate coefficients, and the older atomic data are even up to 50% lower than the present experimental result. This is because strong resonances situated below electron-ion collision energies of 50 meV were underestimated by the theoretical calculation, which also has a severe influence on the rate coefficients in low temperature plasmas. In the temperature range of collisionally ionized plasmas, agreement within 25% was found between the experimental result and the present calculation as well as the calculation by Colgan et al. (2003). The present result constitutes a set of benchmark data for use in astrophysical modeling.

Keywords: atomic process – atomic data – plasma

1. INTRODUCTION

It has been estimated that more than 90% of the visible matter in our universe is in the plasma state (Beyer & Shevelko 2003). Cosmic atomic plasmas are divided into two broad classes (see Savin 2007, for a more in-depth discussion), i): photoionized plasmas, often found in planetary nebulae, X-ray binaries and active galactic nuclei; ii):collisionally ionized plasmas, often found in stars and galaxies. Various types of reactions taking place in astrophysical plasmas, including electron impact ionization, excitation, de-excitation and electron-ion recombination, can result in the emission of radiation. In order to explore the properties of astrophysical plasmas, such as, e.g., charge state distribution, temperature and elemental abundances (Beiersdorfer 2003; Kallman & Palmeri 2007), the X-ray observatories ASCA, Chandra (NASA) and XMM-Newton (ESA), have been launched to observe high resolution X-ray spectra from various cosmic sources (Paerels et al. 2003). To interpret the observed spectra by plasma modeling, accurate atomic data for electron-ion recombination processes, in particular, for radiative recombination (RR) and dielectronic recombination (DR), are crucial for astrophysicists.

The importance of DR in plasma was not appreciated until Burgess first recognized its significance in 1964 (Burgess 1964). Since then, DR has been considered to be a significant electron-ion recombination mechanism, governing the charge state distribution and the temperature in atomic plasmas and contributing to their line emission (Badnell 2007; Savin 2007). Reliable recombination rate coefficients are required for understanding and modeling laboratorial or astrophysical plasmas. Most of the available rate coefficients are from theory. However, the theoretical prediction of DR resonance positions and strengths particularly at low electron-ion collision energies is still a challenging task since an infinite number of states is involved in the DR process and relativistic many body effects should be taken into account in high orders. Presently available atomic structure codes are not able to provide resonance positions in the low energy region with sufficient precision. Unfortunately, small shifts of low energy DR resonance positions can translate into huge uncertainties of the temperature dependent rate coefficient in a plasma. In addition, recent experimental studies of low energy range DR have also shown that results from earlier computations of low-temperature DR rate coefficients are not reliable (Huang et al. 2018). Thus, accurate experimental DR rate coefficients are needed

to benchmark different theoretical approaches and to produce more reliable recombination data. It should be noted that heavy-ion storage rings equipped with electron coolers are presently the only tools to produce reliable low temperature DR rate coefficients with high precision. Previous DR experiments were carried out at the storage rings, i.e., TSR at MPIK in Heidelberg (Schippers 2015), ESR at GSI in Darmstadt, Germany (Brandau et al. 2015), and CRYRING at MSL in Stockholm, Sweden (Schuch & Böhm 2007). More details about DR experiments at the storage rings can be found in a recent review by Schippers (2012) and in the references cited therein.

Calcium is one of the most abundant elements in the solar system (Asplund et al. 2009; Feldman & Laming 2000) and the solar element abundances reflect the element abundances in the universe (Doschek & Feldman 2010). Line emissions caused by $2s2p\ ^1P_1$ - $2s^2\ ^1S_0$ transition of Ca XVII at 192.8 Å were widely observed in X-ray solar flare spectra by the Extreme-Ultraviolet Imaging Spectrometer (EIS) on Hinode (Ko et al. 2009). Observation of the Tycho supernova remnant by XMM-Newton and Cassiopeia A by Chandra have also revealed strong emissions from the calcium ions (Decourchelle et al. 2001; Hwang & Laming 2003). A summary of the spectral lines for Ca XVII can be found in a topical review by Doschek & Feldman (2010) and the atomic data table compiled by Landi & Bhatia (2009). In addition, laboratory study of the spectra of highly ionized calcium in the 100-250 Å range applied to solar flare diagnostics were performed at the TEXT tokamak (Lippmann et al. 1987). Here, we present absolute rate coefficients for electron-ion recombination of Be-like calcium ions from an experiment at the main cooler storage ring CSRm and from the theoretical calculation using the AUTOSTRUCTURE code (Badnell 2011).

For Be-like Ca^{16+}, the most significant recombination channels in the experimental measurement energy range can be expressed as

$$
\begin{aligned}
&\mathrm{Ca}^{16+}(2s^2[^1S_0]) + e^- \rightarrow \\
&\begin{cases}
\mathrm{Ca}^{15+}(2s^2nl) + \gamma, \mathrm{RR}; \\
\mathrm{Ca}^{15+}(2s2p[^3P_{0,1,2};^1P_1]nl)^{**} \rightarrow \mathrm{Ca}^{15+} + \gamma, \mathrm{DR}; \\
\mathrm{Ca}^{15+}(2p^2[^3P_{0,1,2};^1D_2;^1S_0]nl)^{***} \rightarrow \mathrm{Ca}^{15+} + \gamma, \mathrm{TR}.
\end{cases}
\end{aligned}
\tag{1}
$$

Here γ denotes the decay photons. RR is the time reversal of direct photoionization, where a free electron is captured by an ion with emission of a photon simultaneously. DR is a two-step resonant process, in which a free electron is captured by an ion with simultaneous excitation of a core electron, forming a doubly excited ion at first. Subsequently, the unstable intermediate state decays either by autoionization or radiatively. The auto-ionization channel returns the system to the original charge state, whereas the radiative decay, when leading to a state below the ionization threshold, completes the DR process. In Be-like systems, due to the strong correlation between the two bound $2s$ electrons, they can be excited simultaneously forming triply excited $2p^2\ nl$ levels with the initially free electron being captured to an atomic subshell nl. As there are three electrons associated with this process and a triply excited state is formed, it is termed trielectronic recombination (TR). The transition energies and lifetimes associated with the here discussed channels are listed in Table 1.

A number of DR experiments with Be-like ions have been performed at heavy-ion storage rings. Electron-ion recombination rate coefficients of C^{2+}, N^{3+}, O^{4+} (Fogle et al. 2005), F^{5+}(Ali et al. 2013), Ne^{6+} (Orban et al. 2008), Mg^{8+} (Schippers et al. 2004), Si^{10}+ (Orban et al. 2010; Bernhardt et al. 2016), Ar^{14+} (Huang et al. 2017, 2018) and Fe^{22+} (Savin et al. 2006) have been measured as benchmark data for astrophysical plasma modeling. TR was first observed with Be-like Cl^{13+} at the TSR (Schnell et al. 2003), and hyperfine-induced transition rates of Be-like Ti^{18+} and S^{12+} were investigated by means of DR spectroscopy at the TSR (Schippers et al. 2007a,b, 2012). Furthermore, DR spectroscopy was used to investigate quantum electrodynamics (QED) and electron-electron correlation effects in Ge^{28+} and Xe^{50+} (Orlov et al. 2009; Bernhardt et al. 2015).

Here we report the first measurement of the electron-ion recombination spectrum of Be-like Ca^{16+}. This paper is structured as follows: The experimental setup and data analysis are presented in section 2. In section 3, we will give a brief introduction to the theoretical calculations with the AUTOSTRUCTURE code. Results of merged-beam recombination rate coefficients as well as plasma rate coefficients are presented and discussed in section 4. Conclusions are given and the most important results are summarized in section 5.

2. EXPERIMENT AND DATA ANALYSIS

Table 1. Excitation energies and lifetimes of Ca^{16+} levels.

Level	Excitation energy		Lifetime
	NIST[a]	(Wang et al. 2015)	
	(eV)	(eV)	(s)
$1s^22s^2\ ^1S_0$	0	0	∞
$1s^22s2p\ ^3P_0$	32.024	32.0355	2.3[6][b]
$1s^22s2p\ ^3P_1$	33.409	33.4235	1.475[-7]
$1s^22s2p\ ^3P_2$	36.817	36.8259	3.600[-3]
$1s^22s2p\ ^1P_1$	64.301	64.2983	8.948[-11]
$1s^22p^2\ ^3P_0$	85.435	85.4478	1.231[-10]
$1s^22p^2\ ^3P_1$	87.617	87.6299	1.148[-10]
$1s^22p^2\ ^3P_2$	90.068	90.0797	1.146[-10]
$1s^22p^2\ ^1D_2$	98.956	98.9378	3.325[-10]
$1s^22p^2\ ^1S_0$	119.914	119.903	5.736[-11]

[a] Energy levels taken from NIST atomic spectra database (Kramida et al. 2018).

[b] Lifetime associated with the E1M1 two-photo transition is estimated according to the calculated results by Fritzsche et al. (2015).

The experiment was performed at the main cooler storage ring (CSRm) at the Institute of Modern Physics in Lanzhou, China. A detailed description of the experimental setup and the experimental procedures for DR experiments at the CSRm have already been given by Huang et al. (2015, 2018). Here we will only briefly describe the electron-ion recombination experiment with Be-like $^{40}Ca^{16+}$ at the CSRm.

The $^{40}Ca^{16+}$ ions were produced in a superconducting electron cyclotron resonance (ECR) ion source , accelerated by a sector focused cyclotron, and then injected into the CSRm at an energy of 8.42 MeV/u. Every injection pulse of ions was sufficient to provide a maximum ion beam current of

about 90 μA, corresponding to 1.4×10^8 ions stored in the ring. The storage lifetime of the ion beam was about 50 s. During the experiment, the 35 kV electron cooler was employed to maintain the high quality ion beam by means of electron cooling. The electron beam was also used as an electron target in the recombination experiment. In the cooler section, the ion beam was merged with the electron beam over an effective interaction length $L = 4.0$ m. In order to generate a colder electron beam to reach a higher experimental resolution, it was magnetically expanded (Danared 1993). The magnetic fields applied at the cathode and the cooler section were 125 mT and 39 mT, respectively. The expanded diameter of the electron beam was d $\sim$ 62 mm and the electron density in the cooler section was 9.2×10^5 cm^{-3} in the cooler section. The recombined ions formed in the cooling section were separated from the main ion beam in the first dipole magnet downstream from the electron cooler and detected by a movable scintillation particle detector (YAP:Ce+PMT) with nearly 100% efficiency (Wen et al. 2013).

To ensure a high ion-beam quality, the stored ions were electron-cooled for about 2 s after their injection pulses into the storage ring. During the electron cooling, the electron energy was set at the cooling energy of 4.62 keV, which corresponds to zero electron-ion collision energy in the center of mass frame. Offset voltages were applied to the cathode voltage by a suitably designed detuning system to obtain non-zero collision energies. In addition, a DC current transformer (DCCT) was used to monitor the ion beam current and the lifetime of the ion beam in the ring in real time. Two ion beam position monitors (BPM) and one electron BPM were utilized to monitor the spatial overlap of the electron beam and the ion beam in the cooling section. Schottky-noise signals were recorded and analyzed by a Tektronix RSA3408 spectrum analyzer to monitor the revolution frequency and the momentum spread of the ions. The latter was $\Delta p/p \sim 2.2 \times 10^{-4}$.

The absolute recombination rate coefficient as a function of the collision energy can be deduced from the energy dependent detector count rate $R(E)$ as

$$\alpha(E) = \frac{R(E)}{N_i n_e (1 - \beta_e \beta_i)} \frac{C}{L}. \quad (2)$$

Here, N_i is the number of the stored ions in the ring, n_e is the electron density, $C = 161.0$ m and $L = 4.0$ m denote the circumference of the ring and the length of the effective interaction section, respectively. RR and DR evolve from the same initial charge state to the same final charge state and they are indistinguishable quantum mechanically. Therefore, the deduced rate coefficient comprises of these two parts as well as an background resulting from collisions of stored ions with residual-gas particles. In this work, the RR rate coefficient and the background were subtracted by an empirical formula described by Schippers et al. (2000).

The electron-ion collision energy in the center of mass frame was calculated using

$$E_{rel} = \sqrt{m_e^2c^4 + m_i^2c^4 + 2m_em_i\gamma_e\gamma_ic^4(1 - \beta_e\beta_i\cos\theta)} - m_ec^2 - m_ic^2 \quad (3)$$

where m_e and m_i are the electron and ion rest mass, respectively, c is the speed of light, $\beta_e = \upsilon_e/c$ and $\beta_i = \upsilon_i/c$ are the electron and ion velocities in the laboratory frame, and γ_e and γ_i denote the respective Lorentz factors. The angle θ between the electron and ion beam is considered to be zero in the present experiment. Space charge effects were taken into account. Drag force effects were found to be negligible. The measurement covers the electron-ion collision energies in the center of mass frame ranging from 0 to 51.88 eV which corresponds to detuning voltages in the range 0-900 V. In the present experiment, the same power supplies were used as in the recombination experiment with Be-like Ar^{14+} at CSRm. Thus, the experimental energy scale has been recalibrated by a factor of 1.05 in the same manner as described by Huang et al. (2018).

3. THEORY

To fully understand the measured electron-ion recombination rate coefficients, the resonant recombination cross sections were calculated by the distorted-wave collision package AUTOSTRUCTURE (Badnell 2011). AUTOSTRUCTURE is a versatile code that is able to calculate energy levels, oscillator strengths, radiative/autoionization rates, and many other quantities using semi-relativistic kappa-averaged wave functions. The calculations for Ca^{16+} were performed in the same way as for Ar^{14+} (see Huang et al. 2018, for further details). In particular, the core excited energies were ad-

justed to match the spectroscopic values from NIST atomic spectra database (Kramida et al. 2018). Fractions of 95% ground-state ions and 5% metastable ions were assumed in the calculation.

In order to compare the experimentally derived electron-ion recombination rate coefficients with the theoretical calculation directly, the calculated cross sections were multiplied by the electron velocity and convoluted with the velocity distribution of the electrons for the experiment:

$$\alpha(E) = \int_{-\infty}^{+\infty} \sigma(v) v f(v, T_{\parallel}, T_{\perp}) d^3v, \tag{4}$$

where $f(v, T_{\parallel}, T_{\perp})$ is the anisotropic electron velocity distribution, which is characterized by the parallel and perpendicular electron temperatures $k_B T_{\parallel} = 0.8meV$ and $k_B T_{\perp} = 40meV$ (Huang et al. 2015).

4. RESULTS AND DISCUSSION

4.1. *Merged-beam recombination rate coefficients*

The absolute merged-beam recombination rate coefficients for Be-like calcium ions are displayed in Figure 1. The measured spectrum covers the energy range 0-51.88 eV. It contains DR resonances associated with excitation of the $2s^2$ core to the $2s2p\ ^3P_{0,1,2}$ and $2s2p\ ^1P_1$ levels and significant TR contributions. The resonance positions of each Rydberg state can be estimated from the Rydberg formula

$$E_{res}(n) = E_{exc} - R\frac{q^2}{n^2} \tag{5}$$

where $R \approx 13.60569$ eV is the Rydberg constant, $q = 16$ is the primary ion charge state, n denotes the principal quantum number of the captured electron, and E_{exc} is the core-excitation energy. Values for E_{exc} are listed in Table 1 for a number of transitions of interest. The formula works well for high-n resonances where the interaction between the Rydberg electron and the core electrons is very weak. However, the low-n resonance positions are dominated by the complex fine structure of the associated multiply excited configurations. In the storage ring electron-ion recombination experiments at CSRm, the recombined ions traverse one toroidal magnet, three quadrupole magnets and one dipole magnet on their way to the detector. The motional electric fields that the ions experience in these magnets

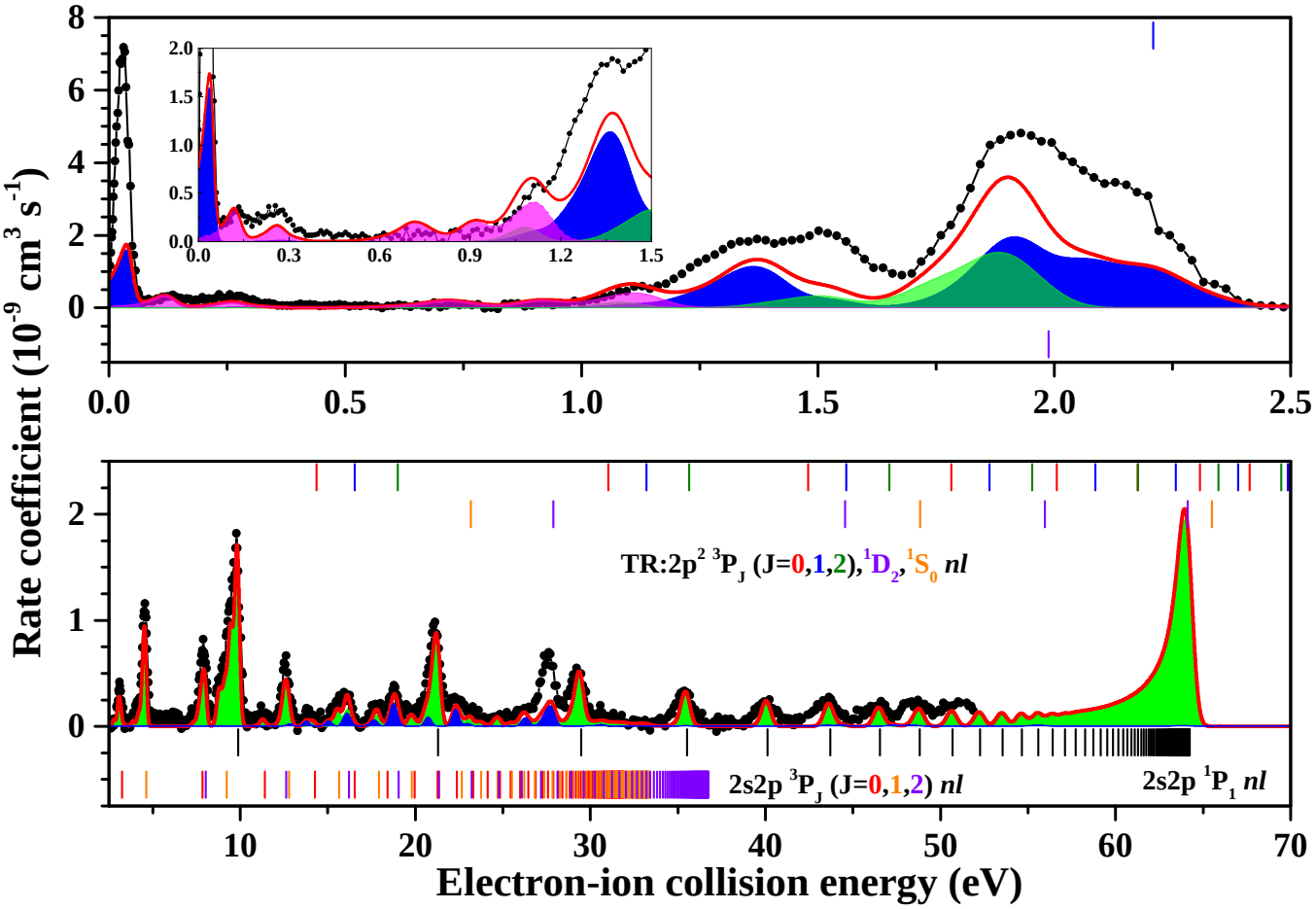

Figure 1. Absolute electron-ion recombination rate coefficients of Be-like Ca as a function of collision energy. The experimental result (the connected filled circles) covers the energy range 0-51.88 eV. The presently calculated field-ionization-free rate coefficient (the red solid line) accounts for fractions of 95% ground-state ions and 5% $2s2p\ ^3P_0$ metastable ions. The pink shaded area shows the rate coefficient originating from the metastable state ions. DR and TR rate coefficients are denoted by shaded green and blue curves, respectively. The vertical bars below the spectra denote the estimated resonance positions (Eq. 5) for the $\Delta N = 0$ series of DR resonances associated with $2s^2\ ^1S_0 \rightarrow 2s2p\ ^3P_{0,1,2},^1P_1$ core excitations. TR resonance positions associated with the $2s^2\ ^1S_0 \rightarrow\ 2p^2\ ^3P_{0,1,2},^1D_2,^1S_0$ core excitations are indicated by the differently colored vertical bars above the spectra.

lead to field ionization of Rydberg electrons with their principal quantum numbers $n > n_{cutoff}$ will be field-ionized at the magnets before being detected. The field-ionized ions cannot be separated from the primary ion beam and, consequently, will not be detected. The cut-off quantum number n_{cutoff} can be estimated by a simple formula (Fogle et al. 2005). However, the present experimental

recombination spectrum does not cover high-n Rydberg levels converging to the $2s2p(^1P_1)$ series limit at 64.301 eV and the $2s2p(^3P_J)$ series limits at about 32-37 eV (Table 1) are not prominently visible, either, such that there are no marked field-ionization effects on the presently measured DR spectrum.

The green shaded area in Figure 1 denotes the calculated $2s^2 \rightarrow 2s2p$ $\triangle N = 0$ DR rate coefficient. It is clear that, the features below 50 meV, around 1.5 eV and 27.5 eV, can not be attributed to DR resonances. It can be seen from Figure 1 that the experimental features agree better with the solid red line which takes TR contributions into account. The first resonances situated below 50 meV, which can be attributed to TR, are significantly stronger than any other resonance feature in the spectrum. The resonance strengths of this feature and of those at around 1.5 eV and 27.5 eV, which are also dominated by TR, are all underestimated by the theoretical calculation. However, the calculated resonance positions fit with the experimental result well. Therefore, the discrepancies between the experimental rate coefficients and calculated result are mainly due to the underestimation of the TR resonance strengths. As described by Schnell et al. (2003), the formation of the intermediate levels depends sensitively on the details of configuration mixing, making the calculation of trielectronic recombination a challenge for atomic-structure theory.

As a Be-like $^{40}Ca^{16+}$ ion with zero nuclear spin, its $2s2p\ ^3P_0$ excited level can only decay to the ground-state by E1M1 two-photon transition (Marques et al. 1993; Cheng et al. 2008; Fritzsche et al. 2015). Correspondingly, the associated lifetime of this state is about 2.3×10^6 s, which is much longer than the experimental timescale. A fraction of the circulating ions in the storage ring were expected to be at the $2s2p\ ^3P_0$ level during the experiment. Ions in other excited levels can decay to the ground-level during the electron cooling delay before the measurement since their lifetimes are rather short compared to the 2 s delay time (see Table 1). The fractions of the long-lived $^3P_0$ metastable level when extracted from an ECR ion source were discussed by Orban et al. (2001). Accordingly, the percentage of the metastable ions decreases with increasing charging state within the Be-like isoelectronic sequence. For example, metastable fractions of 60%, 40%, 35% and 14% were found for C^{2+}, N^{3+}, O^{4+}, and Ne^{6+} ion beams, respectively. Since we also used an ECR ion source to produce a Be-like calcium ion beam, a fraction of 5% metastable calcium ions was estimated.

This corresponds roughly to what was previously assumed for neighboring members of the Be-like isoelectronic sequence of ions such as Ar^{14+} (Huang et al. 2018) and Ti^{18+} (Schippers et al. 2007a). A separate calculation of electron-ion recombination for 5% $2s2p\ ^3P_0$ metastable ions was conducted using AUTOSTRUCTURE code resulting in the pink shaded curve in the inset of Figure 1. It is found that most of the resonance features below 1.25 eV. For an overall comparison with the experimental recombination spectrum shown in Figure 1, the rate coefficients for ground-level and metastable ions were scaled to 95% and 5%, respectively. With this adjustment, the overall agreement between the experiment and theory is satisfactory except for the strong TR resonances as discussed above.

The uncertainty of the measured rate coefficients is estimated to be less than 30% (at a 1σ confidence level), including a 15% uncertainty due to statistics, electron and ion beam current, electron-ion interaction length, the background subtraction, an uncertainty of 5% from the estimated metastable content and an uncertainty of 20% due to the electron density distribution profile and the position of the ion beam in this profile.

4.2. *Plasma recombination rate coefficients*

For the applications in plasma modeling and astrophysics, plasma recombination rate coefficients for the resonant recombination channels are needed. The temperature dependent plasma rate coefficient $\alpha(T_e)$ can be obtained by convoluting the RR-subtracted experimental recombination rate coefficient with a Maxwell-Boltzmann electron energy distribution of temperature T_e (Schippers et al. 2001):

$$\alpha(T_e) = \int \alpha(E) f(E, T_e) dE, \tag{6}$$

$f(E, T_e)$ is the electron energy distribution:

$$f(E, T_e) = \frac{2E^{1/2}}{\pi^{1/2}(kT_e)^{3/2}} \exp(-\frac{E}{kT_e}). \tag{7}$$

Temperature dependent plasma rate coefficient derived from the experimental result and the AUTOSTRUCTURE calculated rate coefficient are displayed in Figure 2. Since the presently measured rate coefficient misses the $^1P_1$ series limit, the measured electron-ion recombination rate coefficient from 42 to 70 eV was replaced by the AUTOSTRUCTURE calculation including the recombination

into states up to $n_{max} = 1000$. It should be noted that the contribution from recombination into resonance levels with $n > 1000$ can be considered to be very small and, thus, be safely neglected. Such a derived plasma rate coefficient is called field-ionization-free plasma recombination rate coefficient. It is shown as a black solid line in Figure 2 and 3. To compare with the theoretical rate coefficients from the literature, the calculated metastable contribution was subtracted from the experimentally derived rate coefficient. The remaining rate coefficient was then renormalized to a 100% ground-level ion beam by dividing it by a factor of 0.95. The dashed and dotted lines in Figure 2 show the DR and TR contributions, respectively. The vertical error bars denote the 30% uncertainty of the measured recombination rate coefficient.

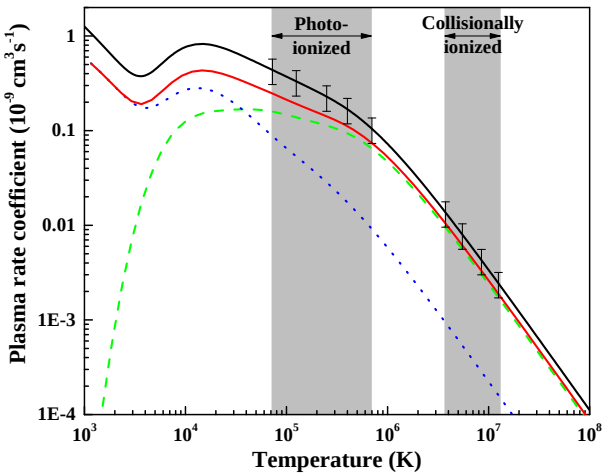

Figure 2. Plasma rate coefficients for DR and TR of Be-like Ca^{16+} as a function of the electron temperature. The solid black line is the experimentally derived $\Delta N = 0$ DR and TR rate coefficients. The theoretical results deduced from the AUTOSTRUCTURE code for $\Delta N = 0$ DR and TR are shown as green dashed line and blue dotted line, respectively. The red solid line is the sum of the calculated DR and TR rate coefficients. The approximate temperature ranges where Ca^{16+} is expected to form in photoionized plasmas and collisionally ionized plasmas are indicated by grey shaded areas and associated arrows (Kallman & Bautista 2001; Bryans et al. 2009). The error bars denote a 30% experimental uncertainty.

The temperature range in Figure 2 is from 10^3 K to 10^8 K. It includes the ranges where Be-like Ca forms in photoionized and collisionally ionized plasmas. The grey shaded areas with associated arrows indicate these temperature ranges. The boundaries of these ranges correspond to the tem-

perature where the fractional abundance of Be-like Ca is 10% of its maximum value Kallman & Bautista (2001); Bryans et al. (2009). TR resonances dominate the rate coefficient for temperatures below 3.5×10^4 K. They play an important role in photoionized plasmas while the TR contribution to the rate coefficient is less than 10% in the temperature range of collisionally ionized plasmas. For temperatures below 5.5×10^4 K where the TR contribution is higher than 40%, the deviation between the experimentally derived plasma rate coefficient and the AUTOSTRUCTURE calculation is more than 45%. Over the temperature range of photoionized plasmas this deviation decreases from 45% to 30% with the decrease of the TR contribution. An agreement of better than 25%, i.e., within the experimental uncertainty is found between the present experimental result and the AUTOSTRUCTURE calculation in the collisionally ionized temperature range. A reasonable explanation is that the theoretical calculation underestimates the TR resonance strengths below 50 meV, around 1.5 eV and 27.5 eV.

For a convenient use of our data in plasma modeling codes, the presently derived plasma rate coefficients were fitted with the function:

$$\alpha(T_e) = T_e^{-3/2} \sum_i c_i \exp(-\frac{E_i}{kT_e}). \quad (8)$$

The fitted values of c_i and E_i are listed in Table 2. The fitted results reproduce the data to within 1% across the entire temperature range of Figure 2. The fitted parameters resulting from the AUTOSTRUCTURE calculation are also presented.

In Figure 3, the experimentally derived field-ionization-free plasma rate coefficient is compared with the theoretically calculated ones from the literature. Results of Jacobs et al. (1980) and Romanik (1988) include DR associated with the $\Delta N = 0$ and $\Delta N = 1$ core transitions. Romanik declared that their results may be incomplete below 8.5×10^4 K for Be-like Ca due to the omission or energy uncertainty of resonances (Romanik 1988). Calculation of $\Delta N = 0$ and $\Delta N = 1$ DR had also been performed by Badnell (1987) and collected by Mazzotta et al. (1998), here we just present the calculated rate coefficient of $\Delta N = 0$ DR. Theoretical calculations by Gu (2003) with the FAC code and by Colgan et al. (2003) with the AUTOSTRUCTURE code provided rate coefficients of $\Delta N = 0$

Table 2. Fitted parameters for the resonant recombination channels derived from the experimental and calculated rate coefficients. The units of c_i and E_i are 10^{-5}cm^{3}s^{-1}K$^{3/2}$ and eV, respectively.

No.	Experiment		AUTOSTRUCTURE (n_{max}=1000)	
i	c_i	E_i	c_i	E_i
1	5.0219	0.55388	3.6230	0.05795
2	6.1690	0.03800	47.571	1.3072
3	260.09	3.2522	151.74	4.8012
4	453.85	1.7154	257.92	2.0015
5	1193.7	9.2268	825.99	10.562
6	2916.7	23.188	1610.5	25.048
7	6298.3	57.720	5795.4	60.088

DR and TR for temperatures from 10^3 K to 10^8 K. It should be noted that the plot of Colgan et al. (2003) as shown in Figure 3 is the revised $\Delta N = 0$ rate coefficients from the OPEN-ADAS website.

For temperatures below 5×10^4 K the calculated plasma rate coefficient by Gu (2003) and Colgan et al. (2003) are more than 45% lower than the experimentally derived one. A probable reason is that the predictions of the low temperature DR and TR rate coefficients are not reliable. The data of Jacobs et al. (1980) are even lower for these temperatures since TR was not included in the calculations. At temperatures about 4×10^5 K, where Be-like Ca is most abundant in photoionized plasmas, the calculated rate coefficients by Gu (2003) and Colgan et al. (2003) are 35% lower than the experimental result. Rate coefficient calculated by Badnell (1987) is about 50% lower than the experimental result since TR was not included in the calculation. The deviation of the theoretical calculated rate coefficients from the experimental results is probably due to the fact that the TR resonances and the low temperature DR resonances can not be calculated with sufficient precision. In the temperature range $4\times10^6 - 1.3\times10^7$ K where Be-like Ca is formed in collisionally ionized plasmas such as solar strong active regions and flares in the upper solar atmosphere. In this temperature range, the calculated data by Badnell (1987) and Gu (2003) are about 35% lower than the experimental

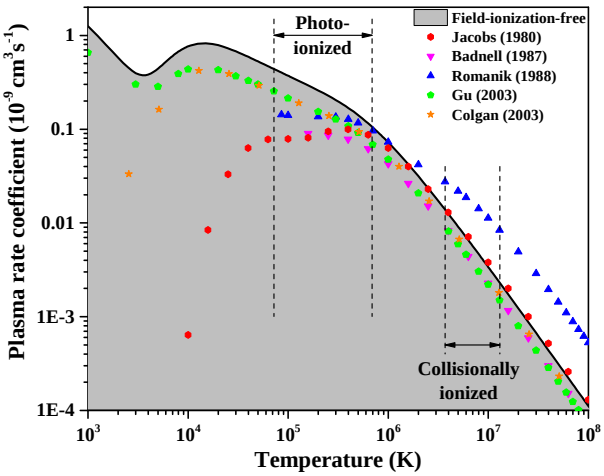

Figure 3. Comparison of the present field-ionization-free resonant plasma recombination rate coefficient (black solid line) with theoretical results for Be-like Ca from the literature. The rate coefficients calculated by Jacobs et al. (1980) and Badnell (1987) are displayed as red hexagons and magenta down-triangles, respectively. The calculations by Romanik (1988) and Gu (2003) are represented as blue up-triangles and green pentagons, respectively. The orange stars show the $\Delta N = 0$ DR and TR rate coefficients calculated by Colgan et al. (2003). The temperature ranges where the abundance of Be-like Ca exceeds 10% of its maximum abundance in photoionized and collisionally ionized plasmas are indicated by vertical dashed lines and associated arrows (Kallman & Bautista 2001; Bryans et al. 2009).

result. An agreement of better than 25% was found between the experimentally derived plasma rate coefficient and the calculation by Colgan et al. (2003). The calculated data of Jacobs et al. (1980) and Romanik (1988) are higher than the experimental data. This is mainly because their calculation included the $\Delta N = 0$ and $\Delta N = 1$ DR while the experimentally derived plasma rate coefficients only include the resonant recombination associated with $\Delta N = 0$ core excitations. The contribution from $\Delta N = 1$ DR cannot be neglected for collisionally ionized plasmas, by 5×10^6 K it is larger than the $\Delta N = 0$, and was accounted-for by Colgan et al. (2003), for example.

5. CONCLUSION

Absolute rate coefficients for electron-ion recombination of Be-like $^{40}Ca^{16+}$ have been measured at the CSRm in the energy range 0-51.88 eV. In addition, theoretical results from the AUTOSTRUCTURE code are presented and compared with the present experimental results. Good agreement was found between calculation and experiment as far as DR resonances are concerned. However,

the calculated TR resonance strengths underestimate the experimental ones, and this translates into a deviation between the experimental and theoretical plasma rate coefficients exceeding the experimental uncertainty. Several resonances originating from the long-lived $2s2p\ ^3P_0$ metastable ions have been identified in the measured spectrum. The calculation for 95% ions in the ground state and 5% ions in the metastable state agrees well with the experimental results for these resonances. The present investigation indicates that the calculation of TR resonances is still a challenging task for the state-of-the-art ATUOSTRUCTURE code while the DR resonances can be calculated with a reasonably high precision.

Experimentally derived field-ionization-free temperature dependent plasma rate coefficients were presented and compared with the available theoretical results. The experimentally derived plasma rate coefficients are higher than the theoretical data in the photoionized zone where TR resonances are important. In a collisionally ionized plasma where Ca^{16+} is most abundant in solar active region and flares, the rate coefficients are dominated by DR resonances, and an agreement of better than 25% is found between the present experimental result and the more recent calculation by Colgan et al. (2003) and the present AUTOSTRUCTURE calculation. Our data provide a benchmark for Ca^{16+} recombination data used in astrophysical modeling.

This work is partly supported by the National Key R&D Program of China under grant No. 2017YFA0402300, the National Natural Science Foundation of China through No. 11320101003, No. U1732133, No. 11611530684, the Strategic Priority Research Program of the Chinese Academy of Sciences, grant No. XDB21030300 and the Key Research Program of Frontier Sciences, CAS, grant No. QYZDY-SSW-SLH006. W. Wen acknowledges the support by the Youth Innovation Promotion Association of the Chinese Academy of Sciences. S. P. Preval and N. R. Badnell acknowledge the support of EPSRC grant EP/L021803/1. S. Schippers gratefully acknowledges support by the CAS President's International Fellowship Initiative (PIFI). The authors would like to thank the crew of the Accelerator Department for skillful operation of the CSR accelerator complex.

REFERENCES

Ali, S., Orban, I., Mahmood, S., Loch, S. D., & Schuch, R. 2013, A&A, 557, A2, doi: 10.1051/0004-6361/201220628

Asplund, M., Grevesse, N., Sauval, A. J., & Scott, P. 2009, ARAA, 47, 481, doi: 10.1146/annurev.astro.46.060407.145222

Badnell, N. R. 1987, JPhB, 20, 2081, doi: 10.1088/0022-3700/20/9/019

—. 2007, JPhCS, 88, 012070, doi: 10.1088/1742-6596/88/1/012070

—. 2011, CPC, 182, 1528, doi: 10.1016/j.cpc.2011.03.023

Beiersdorfer, P. 2003, ARAA, 41, 343, doi: 10.1146/annurev.astro.41.011802.094825

Bernhardt, D., Brandau, C., Harman, Z., et al. 2015, JPhB, 48, 144008, doi: 10.1088/0953-4075/48/14/144008

Bernhardt, D., Becker, A., Brandau, C., et al. 2016, JPhB, 49, 074004, doi: 10.1088/0953-4075/49/7/074004

Beyer, H. F., & Shevelko, V. P. 2003, Series in Atomic and Molecular Physics : Introduction to the Physics of Highly Charged Ions (Iop Publishing Ltd)

Brandau, C., Kozhuharov, C., Lestinsky, C., et al. 2015, PhS, T166, 014022, doi: 10.1088/0031-8949/2015/T166/014022

Bryans, P., Landi, E., & Savin, D. W. 2009, ApJ, 691, 1540, doi: 10.1088/0004-637X/691/2/1540

Burgess, A. 1964, ApJ, 139, 776, doi: 10.1086/147813

Cheng, K. T., Chen, M. H., & Johnson, W. R. 2008, PhRvA, 77, 052504, doi: 10.1103/PhysRevA.77.052504

Colgan, J., Pindzola, M. S., Whiteford, A. D., & Badnell, N. R. 2003, A&A, 412, 597, doi: 10.1051/0004-6361:20031362

Danared, H. 1993, NIMA, 335, 397, doi: 10.1016/0168-9002(93)91223-A

Decourchelle, A., Sauvageot, J. L., Audard, M., et al. 2001, A&A, 365, L218, doi: 10.1051/0004-6361:20000115

Doschek, G. A., & Feldman, U. 2010, JPhB, 43, 232001, doi: 10.1088/0953-4075/43/23/232001

Feldman, U., & Laming, J. M. 2000, PhS, 61, 222, doi: 10.1238/Physica.Regular.061a00222

Fogle, M., Badnell, N. R., Glans, P., et al. 2005, A&A, 442, 757, doi: 10.1051/0004-6361:20040559

Fritzsche, S., Surzhykov, A., & Volotka, A. 2015, NJPh, 17, 103009, doi: 10.1088/1367-2630/17/10/103009

Gu, M. F. 2003, ApJ, 590, 1131, doi: 10.1086/375135

Huang, Z. K., Wen, W. Q., Wang, H. B., et al. 2015, PhS, T166, 14023, doi: 10.1088/0031-8949/2015/t166/014023

Huang, Z. K., Wen, W. Q., Xu, X., et al. 2017, JPhCS, 875, 012020, doi: 10.1088/1742-6596/875/2/012020

—. 2018, ApJS, 235, 2, doi: 10.3847/1538-4365/aaa5b3

Hwang, U., & Laming, J. M. 2003, ApJ, 597, 362, doi: 10.1086/378269

Jacobs, V., Davis, J., Rogerson, J., et al. 1980, ApJ, 239, 1119, doi: 10.1086/158198

Kallman, T., & Bautista, M. 2001, ApJS, 133, 221, doi: 10.1086/319184

Kallman, T. R., & Palmeri, P. 2007, RMP, 79, 79, doi: 10.1103/RevModPhys.79.79

Ko, Y.-K., Doschek, G. A., Warren, H. P., & Young, P. R. 2009, ApJ, 697, 1956, doi: 10.1088/0004-637X/697/2/1956

Kramida, A., Yu. Ralchenko, Reader, J., & and NIST ASD Team. 2018, NIST Atomic Spectra Database (ver. 5.5.2), [Online]. Available: `https://physics.nist.gov/asd` [2018, January 30]. National Institute of Standards and Technology, Gaithersburg, MD.

Landi, E., & Bhatia, A. K. 2009, ADNDT, 95, 155, doi: 10.1016/j.adt.2008.10.003

Lippmann, S., Finkenthal, M., Huang, L. K., et al. 1987, ApJ, 316, 819, doi: 10.1086/165245

Marques, J. P., Parente, F., & Indelicato, P. 1993, PhRvA, 47, 929, doi: 10.1103/PhysRevA.47.929

Mazzotta, P., Mazzitelli, G., Colafrancesco, S., & Vittorio, N. 1998, A&AS, 133, 403, doi: 10.1051/aas:1998330

Orban, I., Böhm, S., Loch, S. D., & Schuch, R. 2008, A&A, 489, 829, doi: 10.1051/0004-6361

Orban, I., Loch, S. D., Böhm, S., & Schuch, R. 2010, ApJ, 721, 1603, doi: 10.1088/0004-637X/721/2/1603

Orban, I., Loch, S. D., Glans, P., Böhm, S., & Schuch, R. 2001, PhS, T144, 014035, doi: 10.1088/0031-8949/2011/T144/014035

Orlov, D. A., Krantz, C., Bernhardt, D., et al. 2009, JPhCS, 163, 012058, doi: 10.1088/1742-6596/163/1/012058

Paerels, F. B., , & Kahn, S. M. 2003, ARA&A, 41, 291, doi: 10.1146/annurev.astro.41.071601.165952

Romanik, C. J. 1988, ApJ, 330, 1022, doi: 10.1086/166531

Savin, D., Gwinner, G., Grieser, M., et al. 2006, ApJ, 642, 1275, doi: 10.1086/501420

Savin, D. W. 2007, JPhCS, 88, 012071, doi: 10.1088/1742-6596/88/1/012071

Schippers, S. 2012, JPhCS, 388, 012010

—. 2015, NIMB, 350, 61, doi: 10.1016/j.nimb.2014.12.050

Schippers, S., Müller, A., Gwinner, G., et al. 2001, ApJ, 555, 1027, doi: 10.1086/321512

Schippers, S., Schnell, M., Brandau, C., et al. 2004, A&A, 421, 1185, doi: 10.1051/0004-6361:20040380

Schippers, S., Bartsch, T., Brandau, C., et al. 2000, PhRvA, 62, 022708, doi: 10.1103/PhysRevA.62.022708

Schippers, S., Schmidt, E. W., Bernhardt, D., et al. 2007a, JPhCS, 58, 137, doi: 10.1088/1742-6596/58/1/025

—. 2007b, PhRvL, 98, 033001, doi: 10.1103/PhysRevLett.98.033001

Schippers, S., Bernhardt, D., Müller, A., et al. 2012, PhRvA, 85, 012513, doi: 10.1103/PhysRevA.85.012513

Schnell, M., Gwinner, G., Badnell, N. R., et al. 2003, PhRvL, 91, 043001, doi: 10.1103/PhysRevLett.91.043001

Schuch, R., & Böhm, S. 2007, JPhCS, 88, 012002, doi: 10.1088/1742-6596/88/1/012002

Wang, K., Guo, X. L., Liu, H. T., et al. 2015, ApJS, 218, 16, doi: 10.1088/0067-0049/218/2/16

Wen, W. Q., Ma, X., Xu, W. Q., et al. 2013, NIMB, 317, 731, doi: 10.1016/j.nimb.2013.07.043